

# Constancy of energy partition in central heavy-ion reactions at intermediate energies

Z Basrak<sup>1</sup>, Ph Eudes<sup>2</sup>, M Zorić<sup>1</sup> and F Sébille<sup>2</sup>

<sup>1</sup> Ruđer Bošković Institute, P.O.Box 180, HR-10 002 Zagreb, Croatia

<sup>2</sup> SUBATECH, EMN-IN2P3/CNRS-Université de Nantes, P.O.Box 20722, F-44 307 Nantes, France

E-mail: basrak@irb.hr

**Abstract.** Semiclassical transport simulation of nucleus-nucleus collisions for the range of incident energy from about the Fermi energy up to a few hundred MeV per nucleon evidences that the maximal excitation energy put into a nuclear system during the early compact stage of heavy-ion reaction is a constant fraction of the center-of-mass available energy of the system. Analysis of experimental data without presuming reaction mechanism dominating the collision process on the best corroborate the found constancy of energy partition in central heavy-ion reactions.

## 1. Introduction

Transformation of the entrance channel longitudinal motion into internal degrees of freedom in the course of heavy-ion reaction (HIR) is still awaiting for a satisfactory answer. With increasing incident energy  $E_{\text{in}}$ , in particular for central collisions, the reaction mechanism evolves from a slow, essentially mean-field–transformation fusion and fusion-like processes to a much faster and considerably more violent reaction mechanism dominated by elementary nucleon-nucleon (NN) collisions. In fusion the entire available energy of the reaction is deposited via thermal excitation, whereas at higher energy a considerable fraction of the available energy is deposited into system via compression. By increasing  $E_{\text{in}}$  one expects that only a fraction of the available energy is effectively deposited into the reaction system and becomes dissipated during the reaction course. It is commonly admitted that this fraction should monotonically decrease with the increase of  $E_{\text{in}}$ .

At  $E_{\text{in}}$  from about the Fermi energy  $E_{\text{F}}$  to about  $100A$  MeV, the energy transformation is determined by those processes which govern heating and compression of a reacting system. In this energy range the time scales involved are rather short and are of the order of time which reaction partners need to bypass each other [1, 2]. Two entrance channel factors play a central role in the determination of the dominant reaction mechanism: projectile energy per nucleon  $E_{\text{in}}$  and reaction geometry (impact parameter and system mass asymmetry). Consequently, the course of a HIR is "decided" in the very first instances of a collision [3, 4]. In central, the most violent collisions the largest fraction of the entrance channel energy is converted into internal degrees of freedom. Thus, the central collisions are of our greatest interest.

We have shown theoretically that an intermediate energy HIR follows a two-stage scenario, a prompt first compact-stage and a second after-breakup one [4]. The emission pattern of central

collisions is characterized by a copious and prompt dynamical emission occurring during the compact and prior-to-scission reaction phase [4–6]. This is the main system-cooling component and the amount of deposited energy into the compact system linearly increases with the projectile energy [7]. These results corroborate conclusion that global characteristics of HIR exit channel are determined in the first prompt reaction stage underlying the interest in studying the first instances of nuclear collisions.

In this work we theoretically examine how much of the system energy may be temporarily stocked into the reaction system in the form of excitation energy as a function of  $E_{\text{in}}$ , system size  $A_{\text{sys}}$  and system mass asymmetry. Four mass symmetric and four mass asymmetric central reactions were studied at several energies (see Tab. 1 for a review). Comparison with the pertinent results deduced from HIR experiments is presented too.

## 2. Theoretical approach

Simulation was carried out within a semiclassical microscopic transport approach of Boltzmann’s type using the Landau-Vlasov (LV) model [8]. The highly nonlinear LV equation

$$\frac{\partial f}{\partial t} + \{f, H\} = I_{\text{coll}}(f) \quad (1)$$

is solved by the test-particle method.  $f(\mathbf{r}, \mathbf{p}; t)$  is the one-body density distribution function describing the spatio-temporal evolution of the system governed by the effective Hamiltonian  $H$  consisting of the self-consistent nuclear and Coulomb fields. The D1-G1 momentum-dependent interaction due to Gogny (the incompressibility module  $K_{\infty}=228$  MeV and the effective mass  $m^*/m=0.67$ ) [9] was used to describe the nuclear mean-field potential.  $\{ , \}$  stands for the Poisson brackets and  $I_{\text{coll}}$  is the collision integral. The effects of the Pauli-suppressed two-body residual NN collisions are treated on average in the Uehling-Uhlenbeck approximation taking the isospin- and energy-dependent free-scattering value for the NN cross section  $\sigma_{\text{NN}}$ . Such an approach is very successful in reproducing a variety of global experimental dynamical observables because they are adequately described by the time evolution of the one-body density. Thus, the LV model is especially appropriate for describing the early stages of HIR, when the system is hot and compressed.

The observable studied is the thermal component (heat), i.e. one of the two main intrinsic-energy deposition components of the early-reaction-stage energy transformation. Heat is stocked into the compact system predominantly by NN collisions which occurs in the overlap zone. This is corroborated by the fact that the Pauli principle greatly favors NN collisions involving one

**Table 1.** Systems and energies studied for central collisions.

System	Incident energy ( $A$ MeV)
$^{40}\text{Ar}+^{27}\text{Al}$	25, 41, 53, 65, 77, 99
$^{36}\text{Ar}+^{58}\text{Ni}$	52, 74, 95
$^{40}\text{Ar}+^{107}\text{Ag}$	20, 30, 40, 45, 50, 75, 100
$^{40}\text{Ar}+^{197}\text{Au}$	50, 75, 100
$^{36}\text{Ar}+^{36}\text{Ar}$	32, 40, 52, 74
$^{58}\text{Ni}+^{58}\text{Ni}$	52, 74, 90
$^{129}\text{Xe}+^{120}\text{Sn}$	25, 32, 39, 45, 50, 75, 100
$^{197}\text{Au}+^{197}\text{Au}$	20, 30, 40, 60, 80, 100

nucleon from the target and one from the projectile. In the most of cases under study the time is too short for the full relaxation of the pressure tensor and establishment of a global equilibrium in momentum space. Therefore, it is more correct to name this component the excitation energy  $E_x$ . Detailed definition of the transformation of the (system) available energy  $E_{\text{avail}}^{\text{c.m.}}$  into intrinsic and collective degrees of freedom may be found elsewhere [7, 10, 11].  $E_{\text{avail}}^{\text{c.m.}}$  is defined as the center-of-mass system energy per nucleon  $E_{\text{avail}}^{\text{c.m.}} = \frac{E_P}{A_P} \frac{A_P A_T}{(A_P + A_T)^2}$ , where  $E_P/A_P = E_{\text{in}}$  and  $A_P(A_T)$  is the projectile (target) number of nucleons.

### 3. Simulation results

As an example of the time evolution of excitation energy per nucleon the inset of Fig. 1 shows  $E_x/A$  for the Au+Au reaction at six energies studied. Within a laps of time of merely 40–75 fm/c after the contact of colliding nuclei occurring at 0 fm/c the excitation energy per nucleon  $E_x/A$  reaches a maximum and then its value decreases almost as rapidly as it increased. As expected, the maxima are reached earlier and their height increases and width decreases with increasing  $E_{\text{in}}$ . The regular and nearly symmetric rise and decrease of  $E_x/A$  with the reaction time is a common behavior for all reactions studied. The observed regularity suggests that maxima of  $E_x/A$  are proportional to the total energy deposited during HIR.

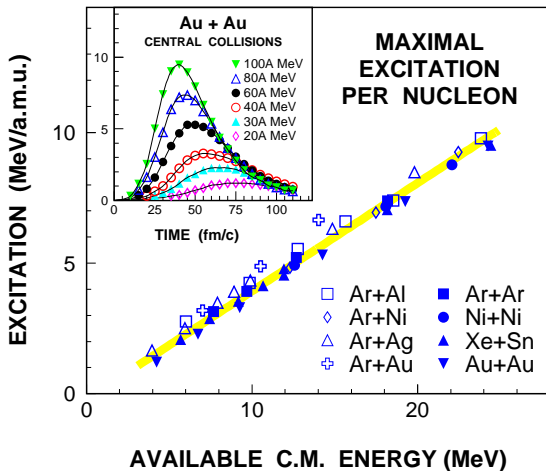


**Figure 1.** (Color online.) Simulation results of the thermal excitation energy per nucleon  $E_x/A$  for central collisions.

*Inset:* Time evolution of  $E_x/A$  for the Au+Au reaction at indicated energies. At each time step considered are particles that are bound in large fragments, in fact the early compact system.

*Main figure:* Excitation maxima  $(E_x/A)_{\text{max}}$  as a function of system available energy  $E_{\text{avail}}^{\text{c.m.}}$  for mass asymmetric (open symbols) and mass symmetric (filled symbols) systems studied. The thick grey line is due to the best linear fit to all data points.

We are examining the maximal energy that may be dissipated in HIR. Thus, we take the maxima of  $E_x/A$  which we denote by  $(E_x/A)_{\text{max}}$ . The value of  $(E_x/A)_{\text{max}}$  can readily and accurately be extracted from the simulation results. Figure 1 depicts how these maxima depends on  $E_{\text{avail}}^{\text{c.m.}}$  for all studied HIR. Abscissa value is shifted for the threshold, the Coulomb barrier energy. With this correction the linear fit over all data points crosses abscissa axis closer to the origin of the graph. All data points lie very close to the fit line. One is facing a peculiar universal linear rise which is independent of  $A_{\text{sys}}$  and mass asymmetry in the full and a rather large span of  $E_{\text{in}}$  covered in this study. The linear dependence of  $(E_x/A)_{\text{max}}$  on  $E_{\text{in}}$  is, of course, present for each individual system studied. Specifying abscissae in  $E_{\text{avail}}^{\text{c.m.}}$  rather than in  $E_{\text{in}}$  merely expresses the mass asymmetric systems on the same footing with those which are mass symmetric.

A universal linear dependence of  $(E_x/A)_{\text{max}}$  on  $E_{\text{avail}}^{\text{c.m.}}$  as well as its nearly exact crossing of the origin in Fig. 1 has an important and remarkable consequence: Expressing the value of maximal excitation in percentage of the system available energy one obtains that the relative fraction of  $(E_x/A)_{\text{max}}$  in  $E_{\text{avail}}^{\text{c.m.}}$  has an almost constant value except for symmetric systems and  $E_{\text{in}} < E_F$ . This departure from the constancy occurs because when  $E_{\text{in}}$  decreases below  $E_F$ <sup>1</sup>

<sup>1</sup> For mass symmetric systems  $E_F$  corresponds to  $E_{\text{avail}}^{\text{c.m.}} \approx 8A$  MeV.

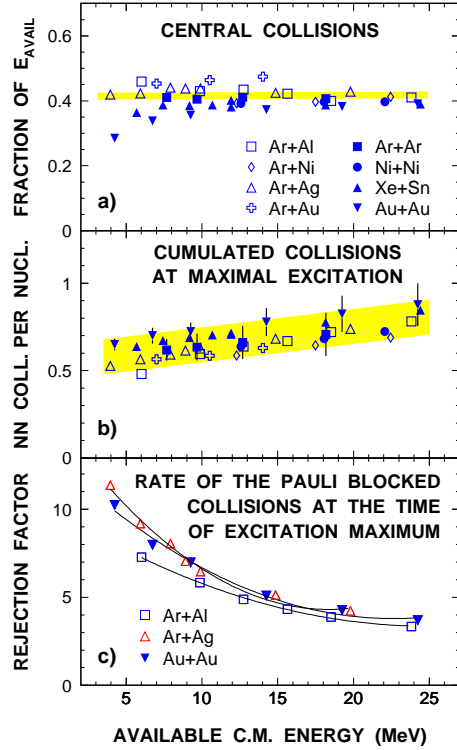


**Figure 2.** (Color online.) *Top*: Ratio of the excitation energy and the corresponding  $E_{\text{avail}}^{\text{c.m.}}$ , as a function of this same available energy  $E_{\text{avail}}^{\text{c.m.}}$ , for the simulation results of Fig. 1.

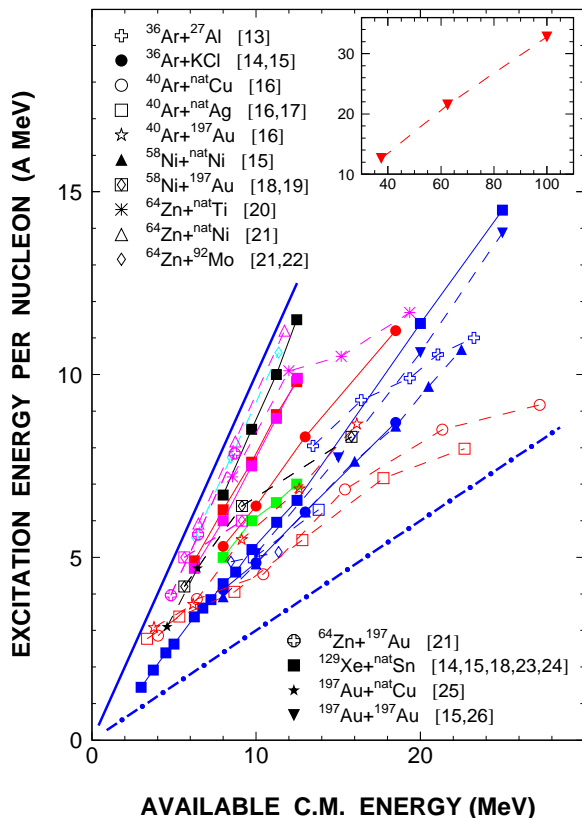
*Middle*: Cumulated average number of NN collisions per nucleon at the time when  $(E_x/A)_{\text{max}}$  is reached.

*Bottom*: The average value of the ratio of the potential to the effectively realized NN collisions per nucleon at the time when  $(E_x/A)_{\text{max}}$  is reached. The curves are due to a parabolic fit and are merely intended to guide the eye.

the value of the maximum  $(E_x/A)_{\text{max}}$  decreases faster than  $E_{\text{avail}}^{\text{c.m.}}$  itself is decreasing. This is a consequence of an ever slower and slower the early compact system energy transformation as  $E_{\text{in}}$  decreases with an ever more broadened maximum (cf. inset in Fig. 1). Therefore, at these lower  $E_{\text{in}}$  the maximum  $(E_x/A)_{\text{max}}$  is no more proportional on the same manner to the total energy deposited in HIR as for  $E_{\text{in}} \geq E_{\text{F}}$ : These  $(E_x/A)_{\text{max}}$  cannot be compared with an experimental  $E_x/A$  of fusion reaction, i.e. of adiabatic-like processes. With this restriction in mind, from Fig. 2a) one infers that share of  $E_x/A$  in  $E_{\text{avail}}^{\text{c.m.}}$  weakly depends on either reaction system or incident energy  $E_{\text{in}}$  and amounts  $0.39 \pm 0.03$  of  $E_{\text{avail}}^{\text{c.m.}}$ . In other words, during the early energy transformation in HIR the maximal excitation energy that may be deposited in the system is a constant which amounts about 40% of the system available energy. As already discussed, this energy dissipation is chiefly owing to NN collisions occurring in the reaction overlap zone. At the time when  $(E_x/A)_{\text{max}}$  takes place the average number of NN collisions per nucleon bound in the compact system for each individual system increases linearly and slowly with  $E_{\text{in}}$  (cf. in Fig. 2b)), whereas Pauli suppression of NN collisions approximately quadratically decreases with  $E_{\text{in}}$  (cf. in Fig. 2c)). In absolute values the above behaviors are within 20% the same for various systems in the energy range studied. With the increase of  $E_{\text{in}}$ , the energy transferred by an individual NN collision and deposited within the overlap zone increases on the average on such a way to remain proportional to  $E_{\text{avail}}^{\text{c.m.}}$ . The observed behavior of energy deposit in HIR is a consequence of these facts. Let us underline that this constancy of the maximum-of-excitation-energy share in available energy is evidenced in the fairly broad range of  $E_{\text{in}}$  (quotient of the highest and the lowest  $E_{\text{avail}}^{\text{c.m.}}$  covered in the simulation is  $\sim 9$ ) and it is nearly independent of system size (studied is the range of  $\sim 60 \leq A_{\text{sys}} \leq \sim 400$  nucleons) and mass asymmetry ( $A_{\text{P}}:A_{\text{T}}$  is varied between 1:1 and 1:5).

#### 4. Comparison with experimental results

An important question is whether the existing central HIR experimental data support our simulation results. Most of the energy put into the system during the early reaction phase is released by the emission of particles and light and intermediate mass fragments owing to the thermal excitation component  $E_x$ . At energies below  $100A$  MeV the compression-decompression process contributes a little in the total (kinetic) energy dissipation in HIR [12]. At the instant at which the maximum  $(E_x/A)_{\max}$  is reached a negligible emission occurs. At energies of our interest it amounts at most 3–5% of the total system mass [7]. Thus, conjunction of the  $(E_x/A)_{\max}$  with the total (kinetic) energy released in HIR seems to be a natural assumption. One must keep in mind, however, that a simulation maximum is reached prior to although very close (of the order of  $\sim 5\text{--}10$  fm/c) to the time at which the total momentum distribution becomes locally spherical, i.e., the instant at which the local equilibrium has been reached in each part of the compact subsystem of bound particles [10]. Nevertheless, the system is far from a global equilibrium [7] and comparison with experimental  $E_x/A$  is not straightforward. In addition, one must bear in mind that one should limit the comparison to general trend of experimental data, i.e. to the possible constancy of  $(E_x/A)/E_{\text{avail}}^{\text{c.m.}}$  as a function of  $E_{\text{avail}}^{\text{c.m.}}$  without seeking to reproduce the simulation absolute value. The maximal excitation share of  $(E_x/A)_{\max}$  in  $E_{\text{avail}}^{\text{c.m.}}$  of 40% is reached during the very first reaction phase and if the same value would be extracted from experimental data that could not but be a fortuitous result. Indeed, experimental data is registered at an infinite time. Hence, it reflects an integral of the full reaction history. Anyway, the simulation maxima  $(E_x/A)_{\max}$  should be compared with either the maximal value of  $E_x/A$  obtained in an experiment or with the most probable value of  $E_x/A$  depending on the nature of the distribution.



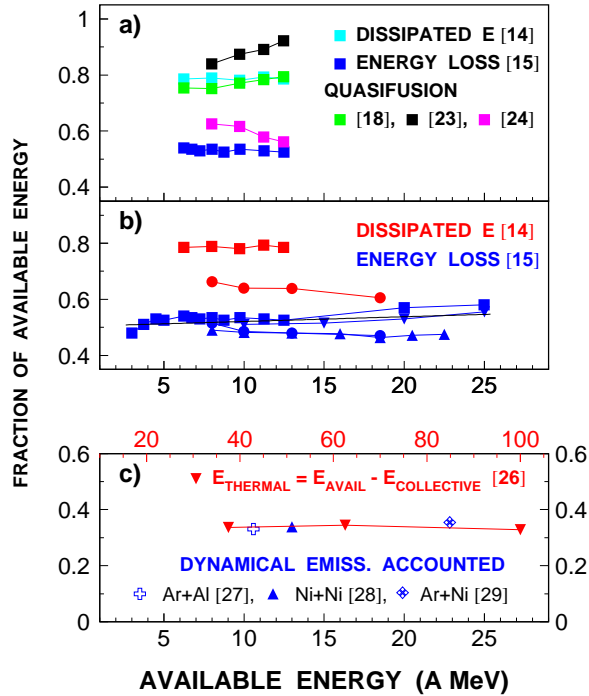
**Figure 3.** (Color online.) Experimentally evaluated total excitation energy per nucleon or total dissipated energy per nucleon as a function of system available energy. Each reaction is represented by its own symbol and by color are distinguished different analyses of the same reaction. The thick full line corresponds to the  $E_{\text{avail}}^{\text{c.m.}}$  and displays the upper energy limit which may be reached in HIR while the thick dash-dotted line depicts 30% of this limit. The only data on total  $E_x/A$  above  $100A$  MeV are for the Au+Au reaction at  $E_{\text{in}}=150A$ ,  $250A$  and  $400A$  MeV [26]. They are shown in the inset. The axes aspect ratio of both the inset and the main diagram is the same so that the slope in both is the same.

Figure 3 displays a collection of experimental data on  $E_x/A$  and total energy dissipated in central HIR published in periodicals during the last two decades [13–26]. Because energy

dependence is crucial for our comparison from the figure are dropped all single-energy results. Each reaction system is depicted by its symbol while the different measurements of the same system are distinguished by color (on line). To avoid of entirely spoiling the figure the error bars, typically of 5–15 %, are not displayed. To guide the eye, points belonging to the same system and the same analysis are connected and they mostly display close-to-linear dependence on  $E_{\text{avail}}^{\text{c.m.}}$ . Unlike the simulation result on  $(E_x/A)_{\text{max}}$  the experimental data points span a large domain of the  $E_x/A$  vs.  $E_{\text{avail}}^{\text{c.m.}}$  plane: The extracted excitations per nucleon lie between one third and almost the full accessible system energy  $E_{\text{avail}}^{\text{c.m.}}$ . One may speculate that the different approaches used in extracting from experiments the pertinent information on the global energy deposition in HIR might be at the origin of these much more scattered results. Indeed, in a HIR experiment one does not have a direct access to the excitation energies involved. To obtain  $E_x/A$  one needs to reconstruct from detected reaction products the total excitation  $E_x$  of an assumed primary emission source but also the source mass  $A$ . There is an evident difficulty to restore the break-up stage using exclusively asymptotic experimental information which is further obscured by an important role played by primary fragments internal excitation causing the in-flight emission. To overcome these uncontrolled issues one has to resort to certain more or less justified physical assumptions or/and to use theoretical predictions as a guide for data analysis. Anyhow, data analyzed on a same footing seems to fall into much narrower zones of the  $E_{\text{avail}}^{\text{c.m.}}$  vs.  $E_x/A$  plane.

Linear dependence of  $E_x/A$  on  $E_{\text{avail}}^{\text{c.m.}}$  is not sufficient to obtain a constancy of its fraction in available energy. For this constancy the line passing through data points should also pass close to the origin of the  $E_{\text{avail}}^{\text{c.m.}}$  vs.  $E_x/A$  plane. As an example in Fig. 4a) are shown results for the Xe+Sn system which have been extensively studied by the INDRA collaboration. Displayed are five analyses of apparently the same data set for  $E_{\text{in}}$  between  $25A$  and  $50A$  MeV [14, 15, 18, 23, 24]. Each analysis have used its own approach in selecting data by centrality and its own philosophy regarding the presumed dominant reaction mechanism used to extract the total excitation  $E_x$  and the primary source mass  $A$ . Reported  $E_x/A$  differ substantially among them. The absolute value at the same  $E_{\text{in}}$  differs up to 80 %. In addition, some of presumed single-source analyses display a rising fraction of  $E_x/A$  in  $E_{\text{avail}}^{\text{c.m.}}$  as  $E_{\text{in}}$  increases [18, 23], other falling fraction as  $E_{\text{in}}$  increases [24], whereas the most probable dissipated energy [14] and the total energy loss [15] displays a weak if any dependence on  $E_{\text{in}}$ . One may argue that various selections of central events may reflect different physics and, thus, have a different  $E_x/A$ . One must admit that reported differences, including rising, steady and falling behavior seems to be too big. This indicates how delicate these analyses are as well as that at least some of them may contain incorrect step(s) in the extraction of the reported values.

Dissipated energy and total energy loss are the analyses inspired by the kinematical arguments and do not require presumption on the dominant reaction mechanism. Their drawback is in their applicability to the mass-symmetric systems only. Figure 4b) displays results for all systems studied by these two approaches in a fairly broad range of  $E_{\text{in}}$ . The total energy loss within the error bars gives the same constant value for all four systems studied. These results are rather weakly depending on  $E_{\text{in}}$  and may be considered constant. Another example of cases with the constant fraction of  $E_x/A$  in  $E_{\text{avail}}^{\text{c.m.}}$  is shown in Fig. 4c). Displayed are three single-energy studies that carefully accounted for the copious midrapidity emission which occurs during the compact and prior-to-scission reaction phase discussed earlier [27–29] as well as the only  $E_x/A$  result reported so far above  $100A$  MeV. Within blast model extracted is the total thermal energy for the Au+Au reaction from  $150A$  to  $400A$  MeV [26]. The abscissae labels above the graph frame are relative to the Au+Au reaction. These Au+Au data have recently been revised [30] but a strict linearity of the studied ratio as a function of  $E_{\text{in}}$  did not change so that the value of our fraction should merely be slightly increased.



**Figure 4.** (Color online.) Ratio of the excitation energy and the corresponding  $E_{\text{avail}}^{\text{c.m.}}$  as a function of this same available energy  $E_{\text{avail}}^{\text{c.m.}}$ . Symbols used to distinguish different systems are the same as in Fig. 3.

*Top:* Five different analysis of the Xe+Sn reaction for  $25A \leq E_{\text{in}} \leq 50A$  MeV.

*Middle:* Ratio values reported in the analyses based on the pure kinematical considerations.

*Bottom:* Ratio values reported in analyses which thoroughly accounted for the pre-equilibrium emission component as well as the results on the total thermal energy reported above 100A MeV and for which the abscissae labels above the graph frame are relative to.

## 5. Conclusions

In conclusion, a semiclassical transport model study of the early reaction phase of central heavy-ion collisions at intermediate energies has been carried out for a variety of system masses, mass asymmetries, and energies below 100A MeV. It has been found that the maxima of the excitation energy  $E_x$  deposited at this early reaction stage into the reaction system represents a constant fraction of about 40 % of the total center-of-mass available energy of the system  $E_{\text{avail}}^{\text{c.m.}}$ . In heavy-ion experiments extracted total dissipated energy per nucleon and total energy loss deduced on kinematical arguments display a similar constancy of their share in the system available energy. A similar result may be found in total excitation energy extracted from experimental observations under condition that the pre-equilibrium emission is properly accounted for. These results indicate that the stopping power of nuclear matter is significant even below the threshold of nucleon excitation and that it does not change appreciably when expressed in units of the center-of-mass available system energy over a wide range of incident energies.

## References

- [1] Durand D, Suraud E and Tamain B 2001 *Nuclear Dynamics in the Nucleonic Regime* (Bristol and Philadelphia: Institute of Physics Publishing)
- [2] Bass R 1980 *Nuclear Reactions with Heavy Ions* (Berlin: Springer)
- [3] Bonasera A, Coniglione R and Sapienza P 2006 *Eur. Phys. J. A* **30** 47
- [4] Eudes P, Basrak Z and Sébille F 1997 *Phys. Rev. C* **56** 2003
- [5] Haddad F, Eudes P, Basrak Z and Sébille F 1999 *Phys. Rev. C* **60** 031603
- [6] Eudes P and Basrak Z 2000 *Eur. Phys. J. A* **9** 207  
Eudes P, Basrak Z and Sébille F 1998 *Proc. 36th Int. Winter Meeting on Nucl. Phys. (Bormio)* ed. Iori I (Milan: University of Milan Press) p. 277
- [7] Novosel I, Basrak Z, Eudes P, Haddad F and Sébille F 2005 *Phys. Lett. B* **625** 26
- [8] Remaud B, Sébille F, Grégoire C, Vinet L and Raffray Y 1985 *Nucl. Phys. A* **447** 555c  
Sébille F, Royer G, Grégoire C, Remaud B and Schuck P 1989 *Nucl. Phys. A* **501** 137
- [9] Dechargé J and Gogny D 1980 *Phys. Rev. C* **21** 1568
- [10] Abgrall P, Haddad F, de la Mota V and Sébille F 1994 *Phys. Rev. C* **49** 1040
- [11] de la Mota V, Sébille F, Farine M, Remaud B and Schuck P 1992 *Phys. Rev. C* **46** 677

- [12] Pochodzalla J 1997 *Prog. Part. Nucl. Phys.* **39** 443
- [13] Péter J *et al.* 1995 *Nucl. Phys. A* **593** 95
- [14] Métivier V *et al.* (INDRA Collaboration) 2000 *Nucl. Phys. A* **672** 357
- [15] Lehaut G 2009 *Ph.D. Thesis* (Université de Caen, Caen, France)
- [16] Rulin Sun *et al.* 2000 *Phys. Rev. Lett.* **84** 43
- [17] Vient E *et al.* 1994 *Nucl. Phys. A* **571** 588
- [18] Borderie B *et al.* (INDRA Collaboration) 2004 *Nucl. Phys. A* **734** 495
- [19] Bellaize N *et al.* (INDRA Collaboration) 2002 *Nucl. Phys. A* **709** 367
- [20] Steckmeyer JC *et al.* 1996 *Phys. Rev. Lett.* **76** 4895
- [21] Wang J *et al.* (NIMROD Collaboration) 2005 *Phys. Rev. C* **72** 024603
- [22] Wang J *et al.* (NIMROD Collaboration) 2005 *Phys. Rev. C* **71** 054608
- [23] Le Neindre N *et al.* (INDRA and ALADIN Collaborations) 2007 *Nucl. Phys. A* **795** 47
- [24] Bonnet E *et al.* (INDRA and ALADIN Collaborations) 2010 *Phys. Rev. Lett.* **105** 142701
- [25] D'Agostino M *et al.* (MULTICS-MINIBALL Collaborations) 2003 *Nucl. Phys. A* **724** 455
- [26] Reisdorf W *et al.* (FOPI Collaboration) 1997 *Nucl. Phys. A* **612** 493
- [27] Lanzañò G *et al.* (ARGOS Collaboration) 2001 *Nucl. Phys. A* **683** 566
- [28] Thériault D *et al.* (INDRA Collaboration) 2005 *Phys. Rev. C* **71** 014610
- [29] Doré D *et al.* (INDRA Collaboration) 2000 *Phys. Lett. B* **491** 15
- [30] Reisdorf W *et al.* (FOPI Collaboration) 2010 *Nucl. Phys. A* **848** 366